YEAST PROTEOSTASIS UNDER ACUTE STRESS

by
Erli Jin

A thesis submitted to Johns Hopkins University in conformity with the requirements for the degree of Master of Science in Engineering

Baltimore, Maryland

April, 2017

Abstract

Protein homeostasis (proteostasis) is crucial to maintain normal cell activity. Loss of proteostasis is related to cell dysfunction and many neurodegenerative diseases. Protein aggregation is a sign of proteostasis loss. In this study, Saccharomyces cerevisiae(budding yeast) is used to study cell proteostasis under acute stress. After heat shock, misfolded proteins in yeast cells form cytosolic aggregates. An affinity based purification method based on model stress protein firefly luciferace towards aggregates is used and the component of aggregates is analyzed using MudPIT. Validation of the proteomics data showed most of them are cytosolic proteins and enrichment in mitochondria compartment. Imaging cells expressing split GFP showed aggregates go to mitochondria after heat shock and degraded by mitochondria. Disruption of mitochondria protease slow down aggregates dissolution. Disease related protein like TDP43 and α-synuclein are also related to mitochondria.

Advisor: Prof. Rong Li

Thesis Reader: Dr. Petr Kalab

Acknowledgments

I would like to first thank my advisor, Dr. Rong Li for her mentorship. For a student new to the field, she has been very patient and helpful when I have questions or lack of knowledge. I also want to express my appreciation to Linhao, a PhD student in Dr. Li's lab, for teaching me experimental skills, critical thinking and methods to perform science. I will never forget the days we work together on our paper, tired but enthusiastic. Thanks to all Li lab members for being so helpful and kind. It's really an honor and pleasure to work with you guys.

At last I want to express my gratefulness to my parents for supporting my master's study oversea. I won't achieve this without your encouragement and love.

Table of Contents

List of Tables

List of Figures

Introduction

Proteostasis (protein stasis), including protein biogenesis, transporting, folding and turnover, is crucial to maintain normal cell life. After synthesis, in order to gain biological function, protein need to be folded into native state. Misfolded or damaged protein will be degraded to recycle the biomaterial[1].

The misfolded proteins are problematic because they tend to form aggregates. This is because the originally buried hydrophobic amino acid residues are exposed. Also one aggregating protein species can also influence the aggregation of another protein. Driven by the hydrophobic forces, these proteins form amorphous structure or amyloid (β strand fibrils). A typical form of aggregate prone structure is the polyglutamine (PolyQ) stretch. As shown in the Fig1, the amorphous aggregates and amyloid have a rather low energy state, which help them stay stable *in vivo.* There is a huge energy barrier between amyloid fibrils and native or unfolded state. So this aggregation process is usually irreversible. Instead of shifting back to normal state, the misfolded proteins are usually degraded and then recycled.

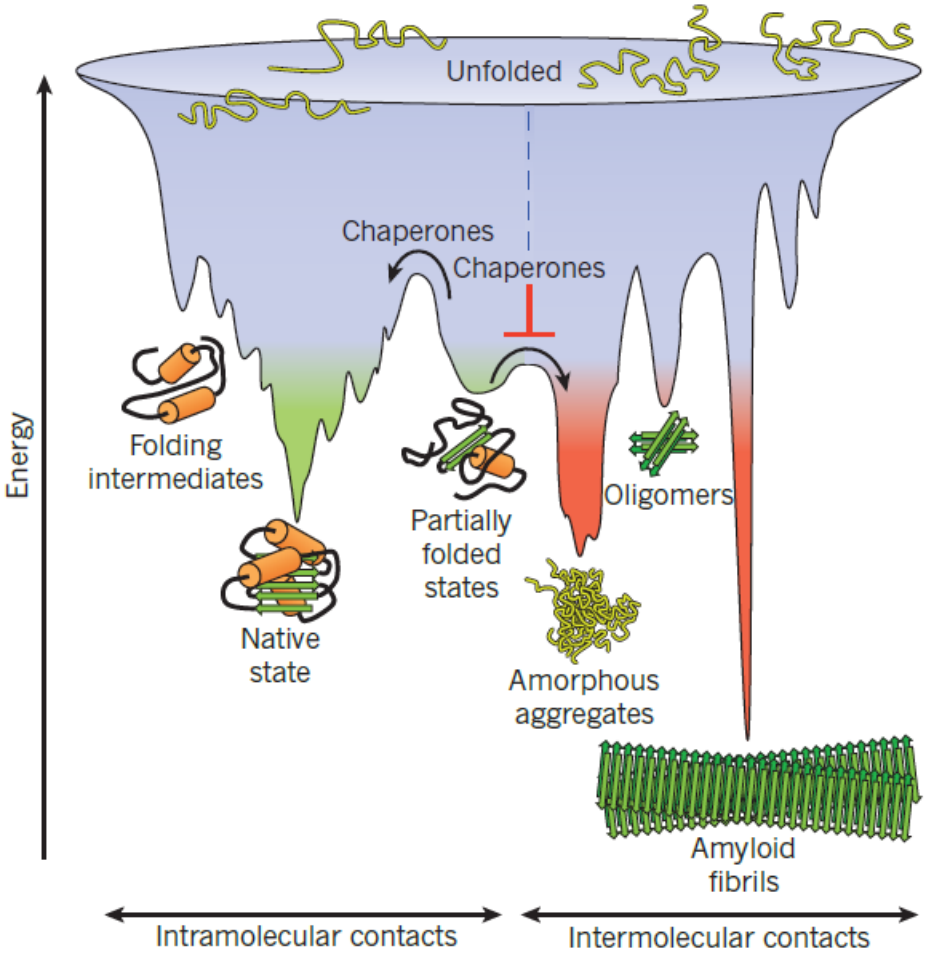

Fig1 Competing reactions of protein folding and aggregation. Scheme of the free-energy surface that proteins explore as they move towards the native state (green) by forming intermolecular contacts. When several molecules fold simultaneously in the same compartment, the free-energy surface of folding may overlap with that of intermolecular aggregation, resulting in the formation of amorphous aggregates, toxic oligomers or ordered amyloid fibrils (red).

The maintenance of the proteostasis is achieved by several protein quality control system[2]. The *de novo* folding or refolding of proteins is regulated by chaperones and its regulators. The breakdown of irreversibly misfolded and aggregated protein includes ubiquitin protease system (UPS)[3] and autophagy system[4]. In eukaryotes, proteasomes are located in the nucleus and the cytoplasm. The main function of the proteasome is to

degrade ubiquitionated unneeded or damaged proteins by proteolysis, a chemical reaction that breaks peptide bonds. Autophagy delivers cytoplasmic constituents to the lysosome. Specialized, cytosolic, double membrane structures that engulf substrates to form autophagic vesicles that ultimately fuse with the lysosome for degradation of their content[3]. It has traditionally been viewed as a rather unspecific degradatin pathway, in which cytosolic contents and organelles are turned over in a non-selective manner.

This form of misfolded protein aggregates is irreversible and its toxicity is related to many neurodegenerative diseases, including Alzheimer's, Huntington's, and Parkinson's[5]. TDP43 is the major disease protein found in the pathological inclusions of two of these diseases, amyotrophic lateral sclerosis (ALS) and frontal temporal lobar degeneration (FTLD)[6]. TDP-43 is a 43 kDa protein ubiquitously expressed in nucleus and undergoes a pathological conversion to an aggregated cytoplasmic localization in affected regions of the nervous system. It provided some molecular similarity between these two disease. Whether TDP-43 itself can convey toxicity and whether its abnormal aggregation is a cause or consequence of pathogenesis remain unknown. Parkinson disease is the second most common neurodegenerative disease. It is characterized by the progressive death of the dopaminergic neurons[7-8]. This associates with a gradual development of symptoms including bradykinesia, muscular rigidity, postural instability, and resting tremor. The molecular hallmark of the disease is the accumulation of proteinaceous inclusions termed Lewy bodies, which contain proteins such as α-synuclein, ubiquitin, synphilin-1, and cytoskeletal proteins[9-10].

In the former study of heat induced aggregates in budding yeast in our group[11], we found that protein aggregates are maintained in the mother cell, preventing them going

into bud. Aggregates are mobile before they bind to certain cell component. Electronic microscopy and super resolution microscopy showed that the aggregates are bind to the mitochondria. Disrupt mitochondria function will slow down the aggregates dissolution.

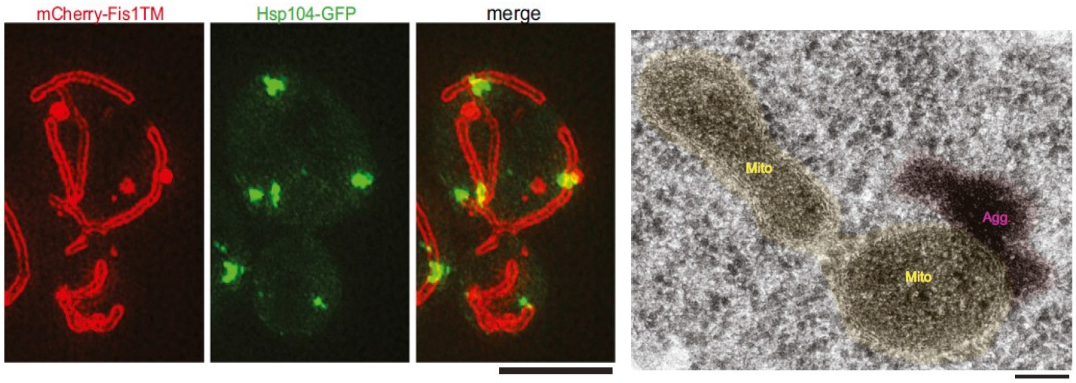

Fig2 SIM images showing association of HS induced protein aggregates (Hsp104-GFP) with mitochondria (labeled with the mitochondria outer membrane marker (mCh-Fis1TM). Scale bar, 4 mm. (B) Thin-sectioning EM images showing association of protein aggregates (magenta) with mitochondria (yellow). Scale bar, 100 nm.

So we want to understand first what the component of the protein aggregates is. Which group of protein prone to form aggregates *in vivo*? Then we also want to know what the relationship between protein aggregates and mitochondria is.

Materials and Methods

Yeast Strains and Plasmids

The yeast strains used in this study are based on the BY4741 background. The GFP, GFP_{11}, HA tagging and knockout are performed using PCR-mediated homologous recombination. The FlucSM construct is based on the plasmid provided by Dr.Hartl[12]. The validation of MudPIT proteomics data was performed from strains from yeast GFP library. The split gfp system was constructed with GFP_{1-10} fused with mitochondria targeting sequence (MTS) and mCherry (MTS-mCherry-GFP_{1-10}) and protein of interest tagged with GFP_{11}. The TDP43 plasmid was a gift from Jiou Wang's lab. In the SIM imaging, the mitochondrial outer membrane was labeled with mCherry-FisTM, GFP_{1-10} was fused with mitochondria matrix protein Grx5 and a native aggregate protein Lsg1 was tagged with GFP_{11}.

Most of the expression plasmids had the p404 backbone and the MTS-mCherry-GFP_{1-10} part was inoculate into Trp locus and the GFP_{11} part was fused into Amp. GFP_{11} replaced GFP in Pfa6a-GFP(S65T)-HIS3MX6 served as universal tagging plasmid. Kan MX was used as a common knockout marker.

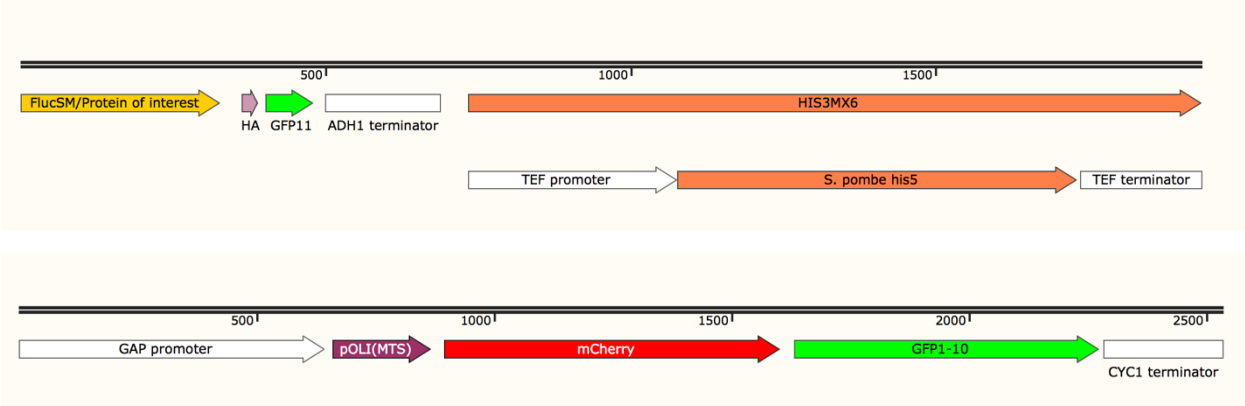

Fig 3 Split GFP system construct. Both FlucSM and mts-mCherry-GFP_{1-10} construct are under GAP promoter. HA-GFP_{11} part serves as universal tagging to protein of interest.

Protein aggregates purification

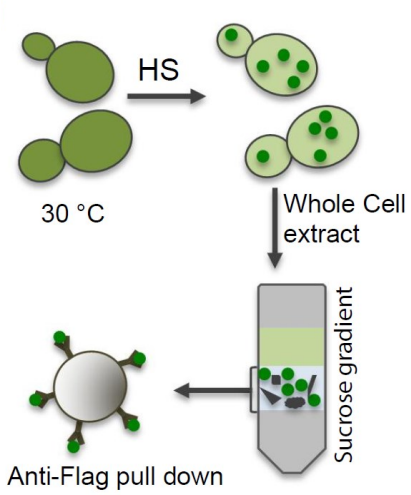

Fig4 Scheme of workflow of aggregates pull down using affinity binding. Green dots represent aggregates forming after HS. Anti-FLAG beads were used to bind concentrated aggregates.

250ml yeast strain (FlucSM-GFP-3xFLAG) was cultured overnight and refreshed to OD600 0.5. After 30 min heat shock (HS) at 42°C (or 15min HS or 0.7mM H_2O_2), the cycloheximide (CHX, 100µg/ml) and CCCP (25µm) were added directly to the culture and mix well for about 2-3min before centrifuge[13].

Cells were collected by centrifugation (5000g 4min) and then washed once with water, separated into two 2mL tube, followed by 10mM DTT treatment for 5min (PH 9.3) at 30°C. Then cells were washed with sorbitol buffer (PH 7.5, 1.2M Sorbitol) followed by 5min digestion with 0.65mg/mL zymolase in 1mL zymolase buffer (1.2M sorbitol, 1mM KPi, pH 7.5) in each tube. Zymolase was washed away by two run of zymolase buffer after digestion to reduce the amount of protease introduced by zymolase. Each tube lysed with about 700ul lysis buffer (50mM HEPES PH 7.5, 150mM NaCl, 1mM DTT, 5% glycerol, 1% Triton-X100 and protease inihibitor cocktail (Roche mini tablet)) by vortex

and pipetting. After centrifugation at 4°C, 800g for 2 min to remove the large debris, another run of 6000g centrifuge was applied for 1min. Then I recycle about 900ul soup in total.

The soup was carefully loaded onto the sucrose gradient freshly prepared (0.65mL 50%, 2mL 20% and 1 mL 10% sucrose, prepared with lysis buffer (with detergent and glycerol). Start vacuum then 16min centrifuge with 20,000xg at Beckman Optima using swing-out rotor. 18-gauge needle is used to insert into 20% sucrose fraction from the side of centrifuge tube. The bottom part of 20% has the majority of the aggregates that I collect about 900ul.

600µl M2 resin was used. The entire 900ul 20% fraction was directly run through twice under 4°C. Then the resin was immediately washed (9mL TBS) for 10 times. Before elution, 1-2mL TBS was applied to flush resin in order to get rid of clog. For SDS elution, the beads were eluted with 1-1.5mL SDS (2%, 2 times).

Confocal microscopy

Live cell imaging of yeast was acquired using a Yokagawa CSU-10 spinning disc on the side port of a Carl Zeiss 200m inverted microscope equipped with Hamamatsu C9100-13 EMCCD camera. Z stack has a 0.5µm step size. Yeast cells were grown in synthetic complete(SC) media overnight at 30°C. Then the cells were refreshed for 2-3 hours to OD600 0.3-0.5 and heat shock(HS) was performed at 42°C for 30min. The recovery was performed after HS under 30°C for desired time. All the images were processed with ImageJ form NIH and were scaled with bilinear interpolation.

Split GFP assay and quantification

In yeast, protein of interest was tagged with GFP_{11} at C terminus of its genomic locus in the strain that carries MTS-mCherry-GFP_{1-10}. Yeast cells were grown and imaged as described above. HS was performed at 42 ºC in 4 ml culture for 30 min with shaking of 220 rpm. 1ml of yeast culture was directly taken out and imaged after HS. Post HS cultures were shaking with 220 rpm at 30 ºC when indicated time points were acquired (with new medium were added to the culture to keep the OD600 below 0.5 all the time).

Quantification of split-GFP fluorescence was done using a custom python code, which can be found within the git repository located at https://github.com/chiffa/Chromo_vision/blob/master/Linhao_masks_logic.py. Briefly, after reading the mCherry and GFP channel z-stacks, the intensities were summed along the z-axis. The resulting 2D image in the GFP channel was then subject to the random walk segmentation in order to segment out the yeast cells from background and watershed segmentation to separate adjacent cells. The segmentation algorithms were taken from the scikit-image library. Following the segmentation, the median GFP and mCherry intensity in each cell was calculated. Cells whose median GFP is significantly superior to the five cells with lowest GFP in the image are eliminated from further analysis, since they correspond to auto-fluorescence of dying cells. For each cell, mCherry channel was thresholded at 5% of maximal value in order to detect the mitochondria, and median GFP intensity within mitochondria was calculated. This median GFP intensity and mCherry intensity were used in the following analyses.

For yeast quantification of fraction of cells that had the split-GFP signal, all images were acquired with same microscopy setting. Different time points of each sample were set with the same minimum and maximum display value. Maximal z-projection images

were used to count the number of total cell and cells with distinct split-GFP that co-localize with mitochondria mCherry. At least 20 images (more than 350 total cells) from 3 different experiments were quantified at each time point. Worth noting is that, when using cells recovered from frozen glycerol stocks, about 5% of yeast in FlucSM-GFP_{11} showed nuclear GFP signal, but not mCherry signal. Those cells were eliminated from quantification in both cell counting and GFP/mCherry intensity ratio quantification.

Mitochondria Purification

Mitochondria purification was based on a previous protocol[14]. Briefly, yeast cells expressing MTS-mCherry was cultured in 10 liter lactate medium (3 g/L yeast extract, 0.5 g/L glucose, 0.5 g/L CalCl2, 0.5 g/L NaCl, 0.6 g/L MgCl2, KH2PO4, NH4Cl, 22 ml/L 90% Lactic acid, 7.5 g/L NaOH) to OD600 1. Cells were collected by centrifugation and treated with Tris-DTT buffer (0.1 M Tris, 10 mM DTT). After washing with SP buffer (1.2 M Sorbital, 20 mM KPi, pH7.4), cells were treated with 0.5 mg/ml zymolase100T (US biological) at 30 oC for 40 min. Spheroplasts were pelleted, washed with the SP buffer, and then resuspended in regeneration buffer (1.2 M Sorbitol, 1 x Lactate media without glucose) in order to isolate robust mitochondria. Spheroplasts were then washed with the SEH buffer (0.6M Sorbital, 20 mM HEPES-KOH of pH7.4, 2 mM MgCl2, 1 mM EGTA of pH8.0, protease cocktail (P2714, Sigma), PMSF 1 mM was added before use) and broken with a Dounce homogenizer. The homogenate was centrifuged at 1,500 g (low-speed) for 5 min at 4 oC. Supernatant was collected and centrifuged at 12,000 g (high-speed) for 10 min at 4 oC. This step was repeated with resuspending the first low-speed pellet and breaking it with Dounce again. The homogenate was centrifuged with low-speed and high-speed as described above. The

high-speed pellet was collected and the Dounce homogenization was repeated twice with a loose-fitting pestle. The final high-speed pellet contained the crude mitochondria and was carefully transferred to a Nycodenz gradient in Beckman 14 x 89 mm Ultra-Clear Centrifuge tubes (344059). The gradient consisted of 2.1 ml 25%, 2.1 ml 20%, 2.1 ml 15%, 2.1 ml 10%, and 2.1 ml 5% Nycodenz from bottom to top. The gradient was ultracentrifuged in a Swinging bucket rotor (Beckman SW41 rotor) for 60 min at 4 oC with speed at 30,000 rpm. Mitochondria were concentrated around 16% Nycodenz and appeared as a wide red-brownish band in the fourth layer counting from the top.

Aggregates were purified based on the method described above but with two changes. First, the strain used here expressed both FlucSM-GFP-3XFKBP-Myc and FlucSM-HA-GFP_{11}. The motif 3XFKBP was originally included because we thought induced binding may be necessary for import of aggregate proteins in vitro, but we found that aggregates naturally bind mitochondria without any artificial method needed (see Fig. 3c). Second, we used the crude aggregate fraction from the sucrose gradient without the affinity purification in order to obtain sufficient free aggregates for the in vitro import assay. The mitochondria import assay in vitro was detailed described previously15. Briefly, purified mitochondria were mixed with aggregates in import buffer (3% w/v Fatty acid-free BSA, 250 mM KCl, 80 mM MgCl2, 2 mM KH2PO4, 10 mM MOPS-KOH, pH7.2, 1 mM ATP, 2mM NADH, 5 mM creatine phosphate, 0.1 mg/ml creatine kinase). Same amount of mixture was taken out at indicated time point and boiled 15 min in SDS gel buffer for immune blot analysis. Mitochondria purification was based on a previous protocol14. Briefly, yeast cells expressing MTS-mCherry was cultured in 10 liter lactate medium (3 g/L yeast extract, 0.5 g/L glucose, 0.5 g/L CalCl2, 0.5 g/L NaCl, 0.6 g/L MgCl2,

KH2PO4, NH4Cl, 22 ml/L 90% Lactic acid, 7.5 g/L NaOH) to OD600 1. Cells were collected by centrifugation and treated with Tris-DTT buffer (0.1 M Tris, 10 mM DTT). After washing with SP buffer (1.2 M Sorbital, 20 mM KPi, pH7.4), cells were treated with 0.5 mg/ml zymolase100T (US biological) at 30 oC for 40 min. Spheroplasts were pelleted, washed with the SP buffer, and then resuspended in regeneration buffer (1.2 M Sorbitol, 1 x Lactate media without glucose) in order to isolate robust mitochondria. Spheroplasts were then washed with the SEH buffer (0.6M Sorbital, 20 mM HEPES-KOH of pH7.4, 2 mM MgCl2, 1 mM EGTA of pH8.0, protease cocktail (P2714, Sigma), PMSF 1 mM was added before use) and broken with a Dounce homogenizer. The homogenate was centrifuged at 1,500 g (low-speed) for 5 min at 4 oC. Supernatant was collected and centrifuged at 12,000 g (high-speed) for 10 min at 4 oC. This step was repeated with resuspending the first low-speed pellet and breaking it with Dounce again. The homogenate was centrifuged with low-speed and high-speed as described above. The high-speed pellet was collected and the Dounce homogenization was repeated twice with a loose-fitting pestle. The final high-speed pellet contained the crude mitochondria and was carefully transferred to a Nycodenz gradient in Beckman 14 x 89 mm Ultra-Clear Centrifuge tubes (344059). The gradient consisted of 2.1 ml 25%, 2.1 ml 20%, 2.1 ml 15%, 2.1 ml 10%, and 2.1 ml 5% Nycodenz from bottom to top. The gradient was ultracentrifuged in a Swinging bucket rotor (Beckman SW41 rotor) for 60 min at 4 oC with speed at 30,000 rpm. Mitochondria were concentrated around 16% Nycodenz and appeared as a wide red-brownish band in the fourth layer counting from the top.

Aggregates were purified based on the method described above but with two changes. First, the strain used here expressed both FlucSM-GFP-3XFKBP-Myc and FlucSM-HA-

GFP_{11}. The motif 3XFKBP was originally included because we thought induced binding may be necessary for import of aggregate proteins in vitro, but we found that aggregates naturally bind mitochondria without any artificial method needed (see Fig. 3c). Second, we used the crude aggregate fraction from the sucrose gradient without the affinity purification in order to obtain sufficient free aggregates for the in vitro import assay. The mitochondria import assay in vitro was detailed described previously15. Briefly, purified mitochondria were mixed with aggregates in import buffer (3% w/v Fatty acid-free BSA, 250 mM KCl, 80 mM MgCl2, 2 mM KH2PO4, 10 mM MOPS-KOH, pH7.2, 1 mM ATP, 2mM NADH, 5 mM creatine phosphate, 0.1 mg/ml creatine kinase). Same amount of mixture was taken out at indicated time point and boiled 15 min in SDS gel buffer for immune blot analysis.

Results

To study the components of protein aggregates, we used a previously studied model unstable protein, fire fly luciferace carrying a single mutant, tagged with GFP and FLAG (FlucSM-GFP-3XFLAG). The concentrated and purified aggregate protein were analyzed with muti-dimensional protein identification technology (MudPIT)[15]. We totally got 319 candidates of aggregate protein and 245 of the candidates that are available in GFP library[16] were verified using live cell imaging. In detail, the candidates available in the GFP tagging library (with His marker) are streaked out on the SD-His plates. After culture in SC complete media overnight, the cells are refreshed to 0.3-0.5 OD_{600} for 2-3 hours. 1ml culture with or without heat shock at 42°C was taken out and YEP was added to facilitate centrifugation. Concentrated cells were loaded on glass slides covered with 1.5 cover glass. Same laser and camera settings were used to take the images. Each image has more than 10 Z stacks with 0.5 μm step size. As shown in Table.1, 45 percent of the candidates were confirmed forming visible aggregates after HS. Fig.5 shows some examples of aggregates form after HS.

Before HS, the proteins are evenly distributed in the cytosol or certain cell part and after HS they clustered together and form bright punctate. Through the validation, we could see that a majority of them are cytosolic protein in terms of the imaging location. Cytosolic protein, Lsg1, a putative GTPase involved in 60S ribosomal subunit biogenesis, Gpm1, a tetrameric phosphoglycerate mutase and Aph1, dinucleoside triphosphate hydrolase, all form obvious aggregates after HS. At the same time there are also protein located at cell nuclei, membrane and yeast bud neck&tip. For the protein at certain cell

component, most of them translocate to cytosol after heat shock. This is due to the formation of aggregates requires other protein and new protein synthesis[11].

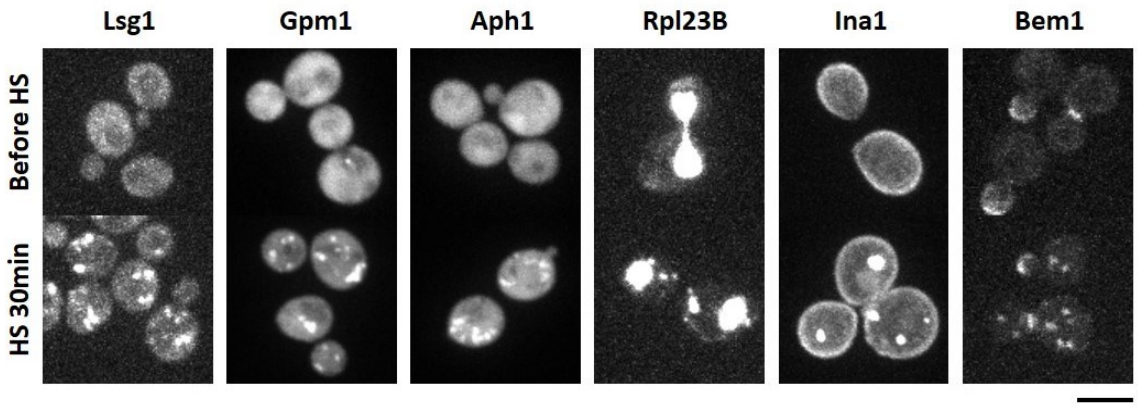

Fig5 Representative images of GFP tagged protein before and after HS. HS: heat shock at 42ºC

Scale bar:5 μm

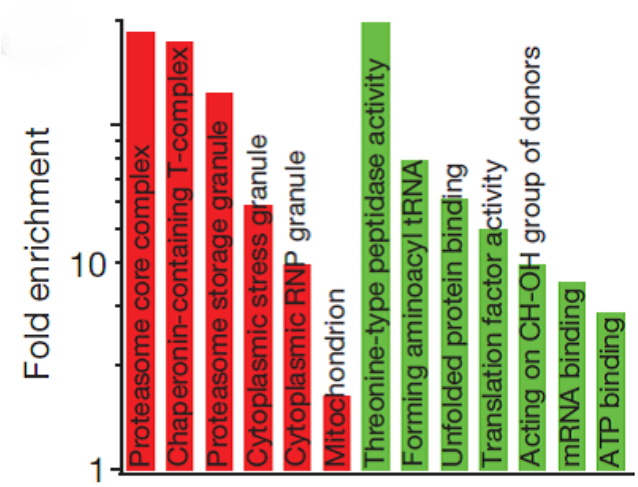

Fig6 Gene ontology analysis for enrichment of aggregate proteins. Green, molecular function; red, cellular components.

Gene ontology analysis[17] revealed most of the candidates are cytosolic proteins and there is an enrichment in mitochondria protein. Mitochondria proteins are known to be unfolded before sent into mitochondria. So there will be a great tendency for them to form aggregates in cytosol. Two component protein of the mitochondria importing

complex[19], Tom70 and Tom40, are also in the list, but they do not cluster together with the aggregates. Aggregates dissolution also seems rapidly delayed by the tim23 temperature sensitive mutant, which disrupts mitochondria inner membrane import complex[11]. Similarly, no mitochondria protein (appeared as mitochondria shape when imaging) formed aggregates after HS. So we hypothesized that the aggregated proteins are imported into mitochondria after acute stress.

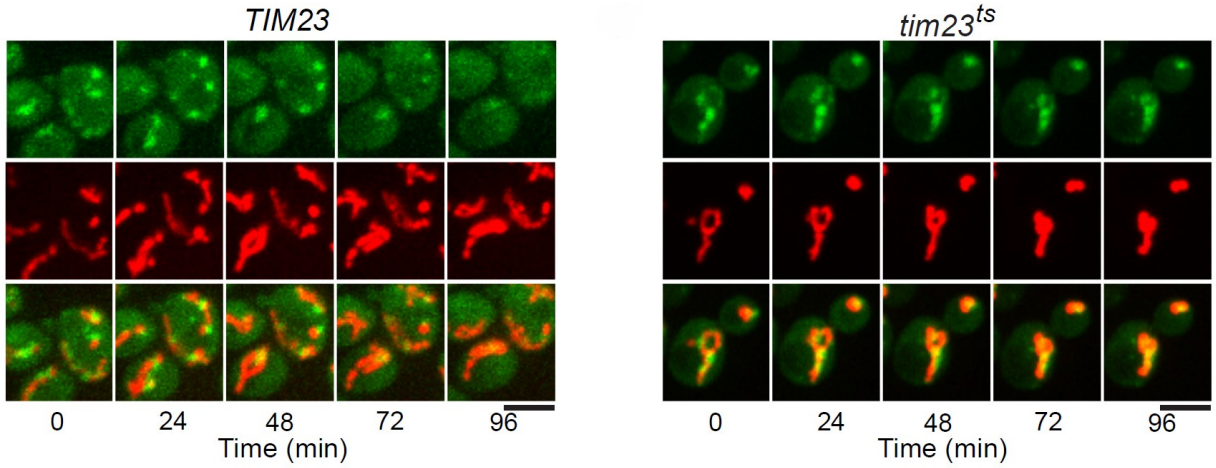

Fig7 Representative images of *TIM23* and *tim23^{ts}* cells from the movies. Aggregates were labeled with Hsp104-GFP (top panels), and mitochondria with MTS-mCherry (middle panels). Bottom panels are merged images. Scale bars, 5μm.

To directly image the entry of misfolded protein into mitochondria, the split GFP system was applied. In brief, the whole GFP has 11βstrands[18]. The GFP_{1-10} was fused to mCherry and mitochondria targeting sequence, which serve as mitochondria marker. The 11th part was tagged to the protein of interest. To test this system, a stable mitochondria matrix protein, GRX5 was tagged with GFP_{11} and showed permanent mitochondria GFP signal before and after HS. A cytosolic protein, HSP104, which will overexpress after heat shock, showed no signal before and after HS. These two experiments serve as positive and negative control. Then the model protein FlucSM tagged with GFP_{11} showed no GFP signal before HS and apparent mitochondrial signal after HS. To further confirm

the protein actually goes into mitochondria, we used the SIM technology. In this case, the mCherry was fused with FIS trans-membrane domain and the GFP_{1-10} part was tagged to GRX5. A native protein, LSG1, which we confirmed forming aggregate after HS, was tagged with GFP_{11}. After HS, the image shows nice mitochondria membrane structure and the GFP signal was inside the membrane layer.

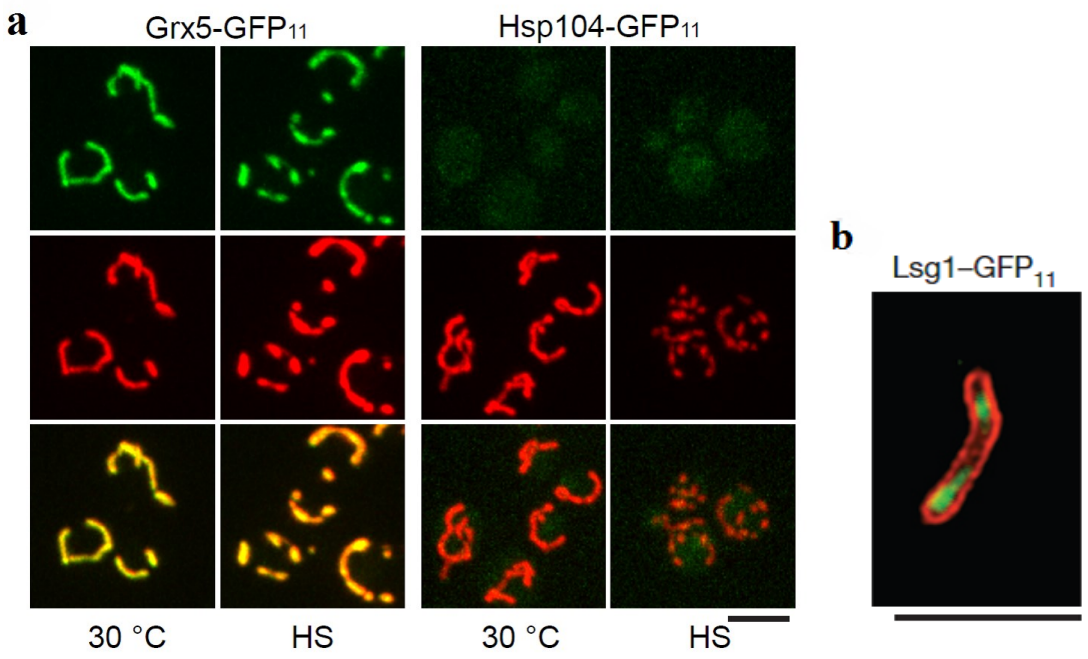

Fig8 Positive (Grx5) and negative (Hsp104) controls used for the split-GFP assay. Top panels: split GFP images; middle panels: MTS-mCherry-labeled mitochondria; lower panels: merged images. (b) Max projected SIM mage of yeast mitochondria. Red: mCherry-Fis1TM. Green: Grx5-GFP_{1-10} and Lsg1-GFP_{11} Scale bars, 5μm.

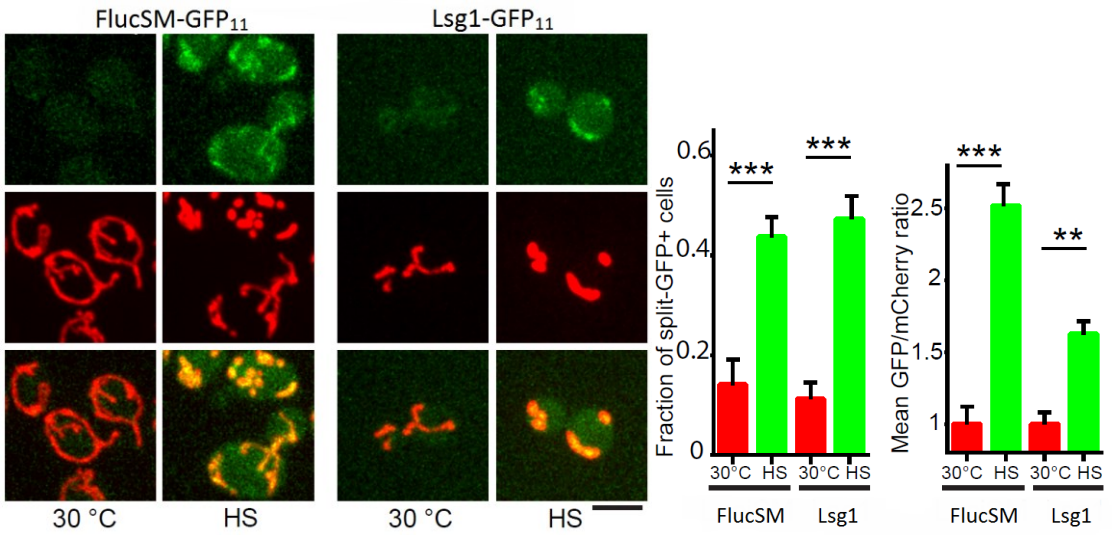

Fig9 Split GFP image and quantification of protein FlucSM and Lsg1 showing the increasing mitochondria GFP signal after HS. Red: mts-mCherry; Green: FlucSM-GFP$_{11}$ and GFP$_{1-10}$ Scale bars, 5μm.

The split-GFP signal of the imported aggregate proteins gradually disappeared in a time course consistent with the dissolution of cytosolic aggregates. This suggests that degradation of aggregate proteins imported into mitochondria may accompany aggregate dissolution. To test this in a biochemical way, we purified mitochondria from yeast culture and crude aggregates from FlucSM-GFP$_{11}$ strain and cultured them together for different time with peptide protease inhibitor cocktail. *In vitro*, aggregates and mitochondria cluster together, consistent with their tight association observed *in vivo*. Increasing incubation time with mitochondria caused more FlucSM-HA-GFP$_{11}$ degradation, as shown by the gradual decrease of full-length FlucSM-HA-GFP$_{11}$ accompanied by the increase in the level of a cleavage product containing the HA epitope in the reactions containing mitochondria but not the ones without. CCCP[20] which is a drug that interfere with mitochondria membrane potential and block import, delayed the degradation of protein aggregates.

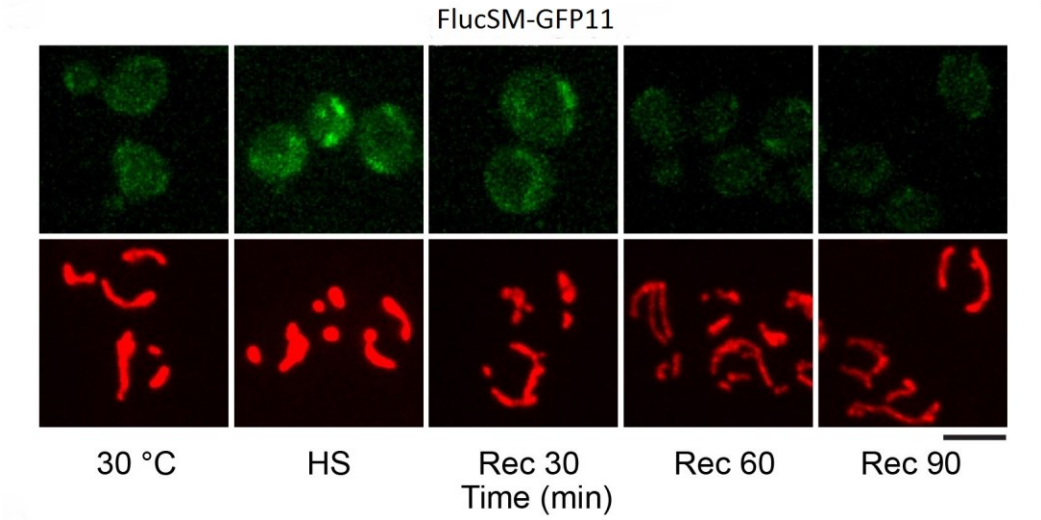

Fig10 Time course imaging shows the dissolution of split GFP signal of FlucSM in mitochondria. Red: mts-mCherry; Green: FlucSM-GFP_{11} and GFP_{1-10} Scale bars, 5μm.

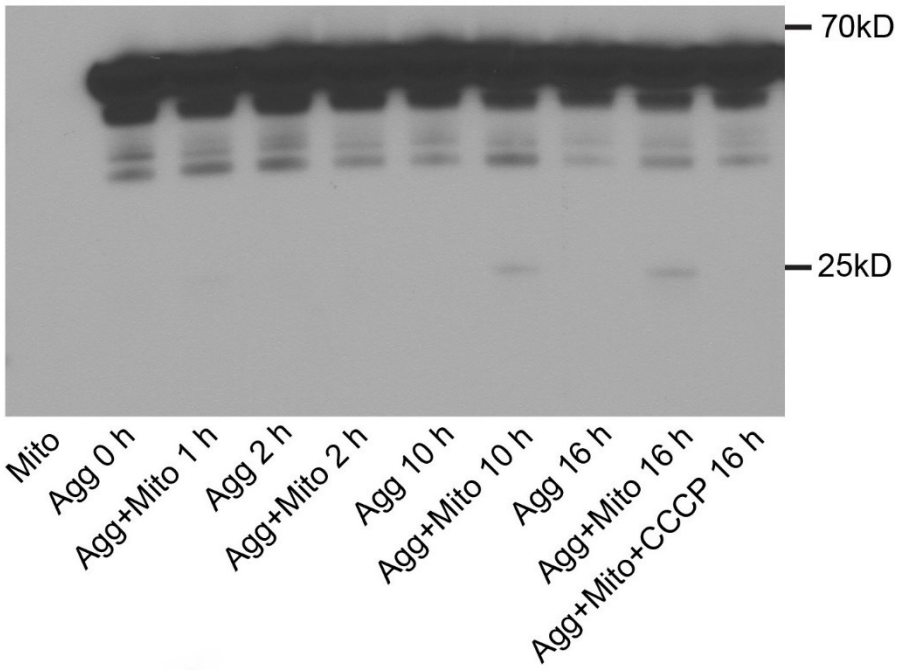

Fig11 Western blot of aggregates incubated with mitochondria with increasing time of incubation.

Proteostasis in yeast mitochondria is governed by 14 mitochondrial proteases, processing peptidases or oligopeptidases[21]. We tested individually the effect of deletion of each of these genes on the dissolution of heat-induced cytosolic aggregates. Compared

to wt, the deletion strains showed modest to strong reduction in the rate of dissolution of cytosolic aggregates, and among them deletion of PIM1[22], encoding a LON protease, and IMP1 and IMP2, encoding mitochondrial inner-membrane peptidases, showed the strongest inhibitory effect. Because Pim1 is a multifunctional protein affecting mitochondrial biogenesis and genome maintenance, to bypass general mitochondria abnormalities in Pim1 knockout cells, we put the pim1S1015A mutant under the same promoter as the original PIM1 gene. The Pim1 protein form a dimer after folding so any dysfunctional mutant will affect the proteolytic activity of Pim1. In this mutant, mitochondrial morphology and general import appeared normal, but the disappearance of FlucSM split-GFP signal in mitochondria during recovery after HS was delayed compared to wt cells. This suggest that disrupt mitochondria protein degradation system could affect the cell proteostasis.

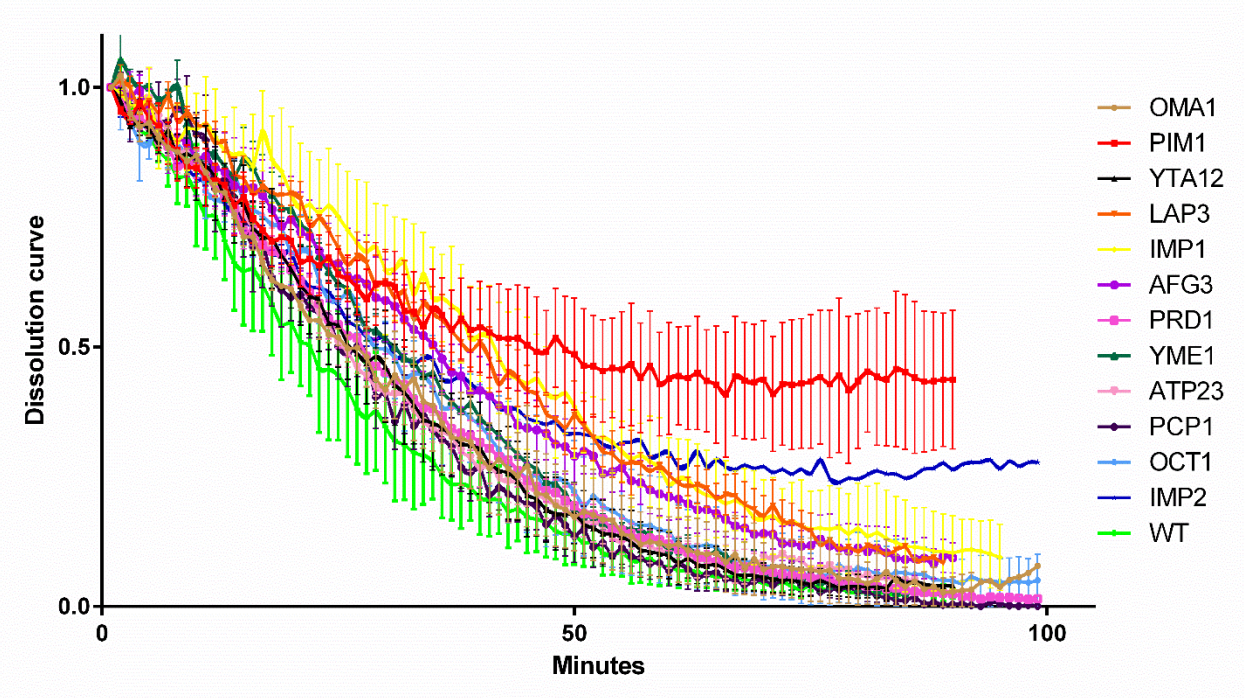

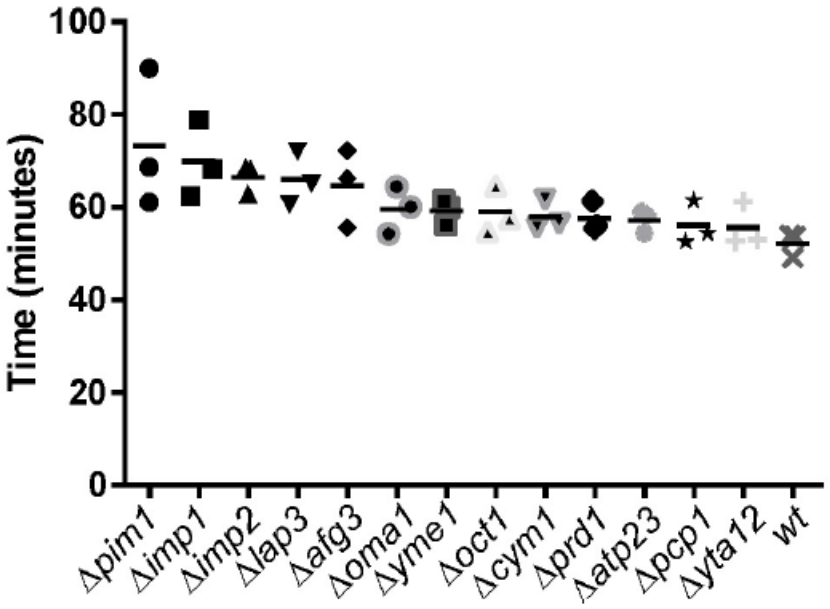

Fig12 dissolution curves of aggregates and the half-decay time of the aggregates showing that the deletion of different mitochondrial proteases delayed the dissolution of cytosolic protein aggregates. Shown in (**c**) are the mean and SEM of normalized aggregates intensities from 3 biological repeats for each gene deletion. Shown in (**d**) are half decay times extracted from fitted curves generated by spline fitting of the same 3 biological repeats as in (**c**).

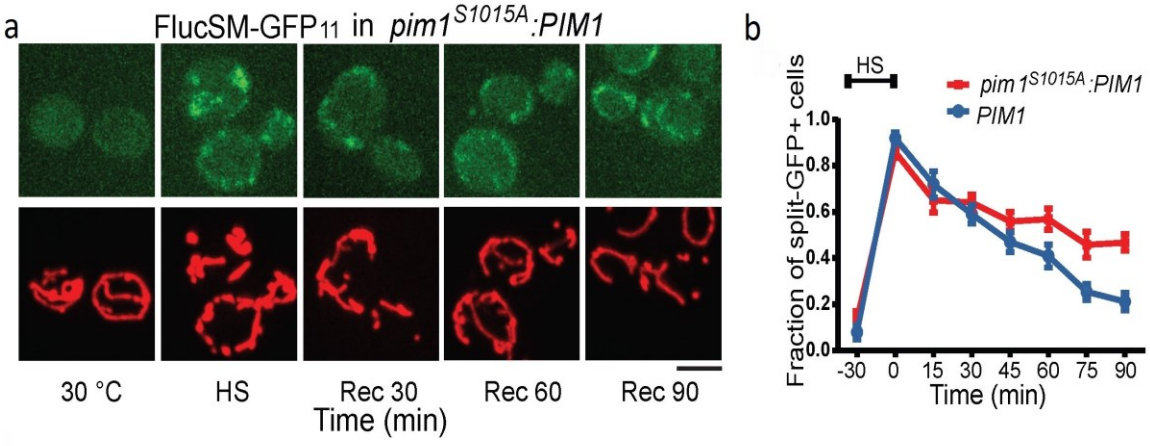

Fig13 **a** Images of FlucSM-GFP$_{11}$ split-GFP signal in *pim1^{S1015A}:PIM1* during recovery after HS. **b**, Quantification of cells with GFP signal in wt(Fig9) and mutant. Shown: mean and SEM Red: mts-mCherry; Green: FlucSM-GFP$_{11}$ and GFP$_{1-10}$ Scale bars, 5μm.

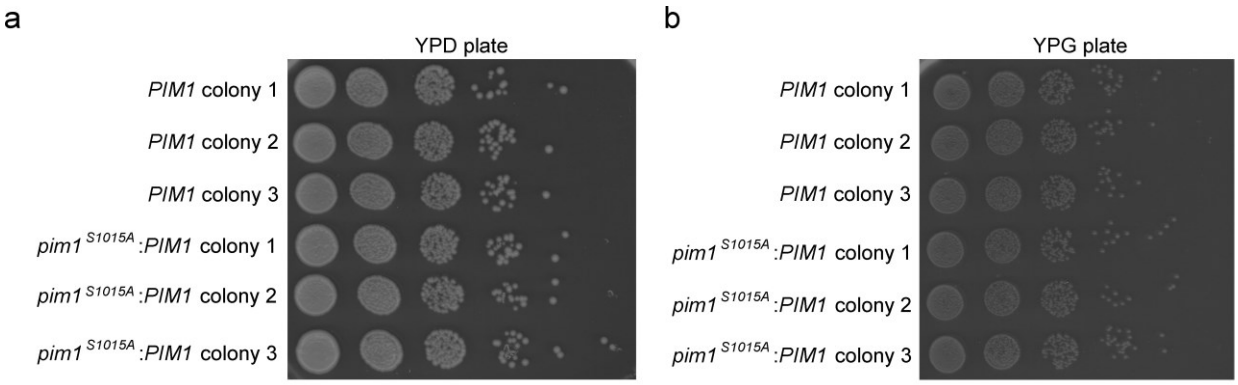

Fig14 Growth assay of wt and *pim1*^{S1015A}*:PIM1* mutant a, b, pim1S1015A:PIM1 grows normally under fermentable (a) and non-fermentable conditions (b).

To study if mitochondria is also related to the typical disease protein, TDP43 and α-synuclein are also put into split GFP system. After heat shock, the TDP43-GFP_{11} strain showed GFP signal colocalized with mitochondria. This suggest that TDP43 may go to mitochondria after heat shock though it is localized to nucleus before HS. In TDP43-GFP cells we did see some dots out of nucleus after HS which is consistent with the former situation. α-synuclein is a membrane binding protein. HS did not change its morphology but it formed several dots and these dots were attached with mitochondria. Through live cell movie, theα-synuclein dots were moving together with mitochondria, which suggest its close relationship with mitochondria. Something interesting to notice is that theα-synuclein split GFP signal also showed the membrane part though the GFP_{1-10} should go into mitochondria. This could be due to the membrane bind property and also the long folding time of mCherry.

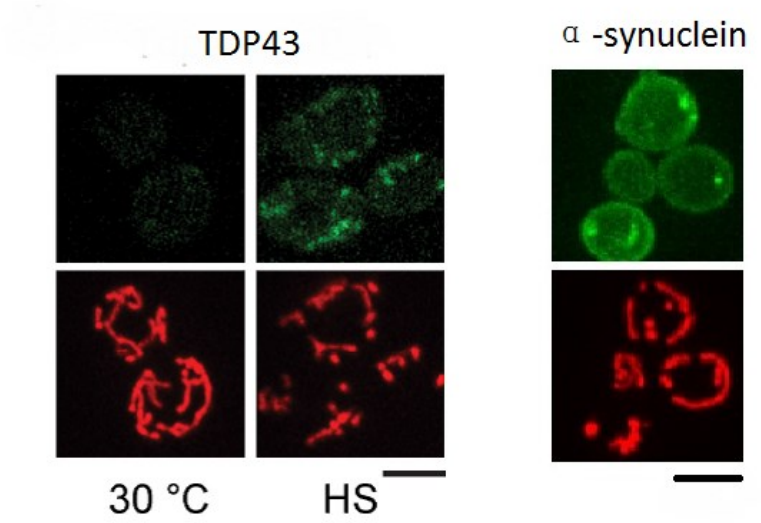

Fig15 Images of TDP43 split GFP and α-synuclein split GFP strain. Red: mts-mCherry; Green: TDP43/α-synuclein -GFP_{11} and GFP_{1-10} Scale bars, 5μm.

Table1

Validation of the proteomic data.

Aggregation: P-have obvious aggregates after HS N-no obvious aggregates after HS

Position: N-nucleus C-cytosol M-membrane Mito-mitochodnria

ORF	Aggregation	Position	ORF	Aggregation	Position
YLR106C	N	N	YDR465C	P	C
YJR137C	P	C	YPR041W	N	C
YDL171C	N	C	YJL026W	P	N
YNR016C	N	C	YOR051C	N	N
YCR093W	N	C	YGR142W	P	C
YPL231W	N	C	YKR048C	N	C
YOR341W	N	N	YJR076C	N	M
YDR150W	N	M	YMR235C	N	C
YKL182W	N	C	YGL048C	N	N
YGL195W	P	C	YGR210C	N	C
YJL130C	P	C	YCR012W	N	C
YDL140C	N	N	YHR179W	N	C
YJR031C	P	C	YPL028W	P	N
YGR271W	P	C	YBR233W	P	C
YPL082C	N	N	YOL022C	P	C
YGL206C	P	C	YHR115C	N	C
YDR127W	N	C	YPL048W	P	C
YPR189W	N	C	YGR214W	N	C
YER155C	P	M	YBR025C	P	C
YNL271C	P	M	YDR161W	P	C
YGL173C	N	C	YLR291C	P	C
YOR207C	N	M	YEL046C	P	C
YBR115C	N	C	YDL168W	N	C
YDR293C	N	N	YKR059W	P	C
YJL074C	P	N	YLR180W	N	C
YOR151C	N	N	YGR185C	N	C
YGR061C	P	C	YGR187C	N	C
YLR398C	N	N	YHR068W	P	C
YMR304W	N	C	YLR244C	P	C
YPL226W	N	M	YDR502C	P	C
YMR012W	N	C	YAL012W	P	C
YLR384C	N	N	YOR063W	N	C
YPR010C	N	C	YDL055C	N	C
YML117W	P	C	YGL105W	P	C
YLR249W	N	C	YGR173W	P	C
YOL098C	P	C	YIR026C	P	C
YGR094W	N	C	YGL148W	P	C
YGL207W	N	N	YAL036C	N	C

YER110C	P	N	YDL188C	P	C
YBL076C	P	C	YLR420W	N	C
YKL205W	N	C	YDR171W	P	C
YJR109C	N	C	YDL134C	P	C
YPL115C	P	C	YDR158W	P	C
YML100W	P	C	YBR249C	N	N
YPL160W	N	C	YBR031W	N	C
YMR308C	N	N	YJR148W	P	C
YOR335C	N	C	YOR136W	N	MITO
YPR019W	N	N	YDR012W	N	C
YGL201C	P	C	YMR318C	N	C
YHR073W	P	M	YGR180C	N	N
YGR204W	N	C	YLR270W	N	C
YML111W	P	C	YBR034C	P	C
YBR084W	N	MITO	YGL039W	P	C
YKL210W	N	N	YNL141W	N	C
YGR240C	P		YOR007C	P	C
YMR205C	N	C	YDL078C	N	C
YBR079C	N	C	YBL016W	P	N
YLL026W	P	C	YBR149W	N	C
YLR347C	N	N	YNL007C	P	N
YDR074W	P	C	YJR139C	N	C
YPL126W	N	N	YMR315W	P	C
YNL112W	P	N	YKL060C	P	C
YER070W	N	C	YER016W	P	C
YLL013C	P	C	YGL040C	N	C
YNL313C	P	C	YGL157W	P	C
YKR089C	N	C	YJR105W	P	C
YER047C	P	C	YOR261C	N	N
YBL023C	N	N	YJR009C	N	N
YMR031C	N	M	YIL041W	N	C
YMR049C	N	C	YDR051C	P	C
YCL030C	P	C	YML004C	P	C
YDL126C	N	N	YPL111W	P	C
YNL085W	P	C	YOR142W	N	MITO
YOR133W	N	C	YNL302C	N	C
YMR309C	N	C	YER156C	N	N
YBR172C	P	C	YOL151W	N	C
YLL034C	N	N	YDR044W	N	C
YGL234W	P	C	YHR104W	P	C
YLR397C	N	C	YPL004C	N	M
YOR361C	N	C	YGR086C	P	
YGR264C	N	C	YLR354C	P	N
YGL009C	P	C	YGR192C	P	
YBR094W	N	M	YKL193C	P	N
YER091C	P	C	YLR017W	P	N

YBR102C	N	M	YPR110C	N	N
YGL120C	N	N	YJR070C	P	C
YIL078W	N	C	YCL050C	N	C
YFR009W	N	C	YML073C	N	C
YGR250C	P	C	YCR002C	N	M
YDR001C	N	C	YKL216W	N	C
YPL106C	P		YDL124W	N	C
YDR164C	P	C	YDR353W	N	C
YOR317W	P	M	YIL021W	P	N
YGL245W	N	C	YPL131W	N	C
YDL167C	P	C	YDL076C	N	N
YGL026C	N	C	YFR004W	N	N
YBR238C	N	C	YGR001C	P	C
YMR246W	N	C	YBR160W	P	N
YMR186W	N	C	YNL312W	N	N
YLR452C	P	C	YHR058C	N	N
YGR178C	P	C	YER117W	P	N
YDR211W	N	C	YKL128C	P	C
YFL047W	N	C	YPR069C	N	C
YLR153C	N	N	YJR007W	N	C
YLR143W	P	C	YFR031C-A	N	C
YBL067C	N	C	YNL006W	P	C
YJL101C	P	C	YOL056W	N	C
YKR036C	N	MITO	YPR103W	N	C
YPL043W	N	N	YOR362C	N	N
YER088C	P	N	YPL117C	N	C
YPR074C	N	N	YDR361C	N	N
YNL197C	P	C	YML026C	N	C
YMR108W	N	MITO	YDR429C	N	N
YKL029C	N	MITO	YIL034C	N	M
YBR121C	N	C	YDR098C	N	C
YER049W	P	N	YGR135W	N	N
YBL075C	P	C	YNL108C	P	C
YLL024C	P		YIL053W	N	C
YGL099W	P	C	YER177W	N	C
YDL224C	P	C	YLR059C	P	N
YAL005C	P	C	YKR043C	P	C
YEL060C	P	C	YMR226C	N	C
YER103W	P	C	YCR009C	N	M
YHR114W	N	M	YIL064W	P	C
YLR060W	P	C	YGR253C	N	N
YOR027W	P	C	YLR301W	N	C
YMR092C	N	C	YOL038W	N	N
YML071C	N	C	YDR050C	P	C
YDL229W	N	C	YML092C	N	N

YER036C	P	C	YKL152C	P	C
YJR016C	N	MITO	YHR049W	N	C
YPL208W	N	N	YJL001W	N	N
YNL209W	P		YLR126C	P	C
YCR088W	N	C	YMR230W	P	
YMR250W	P	C	YLR435W	P	N
YLR133W	P	C	YMR038C	N	C
YJR046W	P	C	YAL049C	N	C
YPL184C	P	C	YGL011C	N	N
YLR028C	P	N	YEL038W	P	N
YGR088W	P	C	YMR314W	N	N
YPR145W	N	C	YNL099C	N	C
YER165W	P	C	YER163C	P	C
YMR105C	N	C	YNL010W	N	C
YFR037C	N	N	YOL149W	N	C
YGR124W	N	C	YLR406C	N	C
YLR044C	P		YHR013C	N	C
YML017W	N	C	YJL136C	N	C
YHR064C	P	C	YDR007W	P	C
YLR134W	N	N	YBR261C	P	C
YBR196C	P	C	YDR487C	N	C
YLR259C	N	C	YLR075W	N	C
YHR009C	P	C	YBL057C	N	MITO
YNL077W	N	C	YBR072W	P	C
YBR200W	P	M	YNL036W	P	C
YDL225W	P	M	YKL142W	N	C
YEL015W	P	M	YOR131C	P	C
YER025W	N	C	YLR178C	N	C
YLR432W	P	C	YGL037C	N	M
YER052C	P	C	YGL101W	P	C
YHR137W	N	C	YJR133W	P	C
YNL241C	N	C	YBR052C	N	M
YER090W	N	C	YKR057W	N	C
YMR169C	P	C	YOR367W	N	M
YOR374W	N	MITO	YML028W	P	C
YKL103C	N	C	YPR172W	N	C
YGR155W	N	C	YDR071C	P	C
YKL081W	P	C	YKR035W-A	N	C
YHR170W	N	C	YLR179C	N	C
YOR310C	N	N	YDR032C	N	M
YAL038W	P	C	YLR109W	P	C
YCL040W	N	C	YOL143C	P	C
YHR183W	N	C	YGR085C	N	C
YER133W	N	C	YPL211W	N	N
YNL239W	P	C	YKL056C	P	C

YNL071W	N	MITO	YER150W	N	N
YEL071W	P	C	YDR155C	N	N
YDR516C	P	C	YDR418W	N	C
YPL091W	P	C	YPR062W	P	C
YKL035W	N	C	YLR421C	N	N
YOL061W	N	C	YMR022W	N	N
YDR388W	P	M	YCR028C-A	N	MITO
YGL202W	N	C	YBR244W	N	C
YBR126C	P	C	YBL018C	N	N
YFR053C	N	C	YMR236W	N	N
YPL061W	P		YKL067W	N	C
YGL253W	N	C	YDR224C	N	N
YFR044C	P	C	YPL250C	P	C
YML126C	N	N	YNL135C	N	C
YPL262W	N	MITO	YJL173C	P	N
YER081W	N	C	YKL058W	N	N
YHR018C	P	C	YCR060W	P	C
YNR001C	N	MITO	YLL040C	N	C
YEL047C	N	C	YGL137W	N	C
YLR058C	N	C	YML103C	N	N
YKL145W	N	N	YDL145C	N	C
YDR023W	N	C	YGL008C	P	
YCR005C	P	C	YDR011W	N	M
YMR027W	N	C	YDL185W	N	C
YHL021C	N	MITO	YHR027C	N	N
YPR080W	N	C	YFR030W	N	C
YDL103C	N	C	YHR098C	N	M
YER003C	P	C	YLR413W	P	M
YDR190C	P	N	YLR166C	P	M
YCL037C	N	C	YKR001C	N	C
YML005W	P	C	YJL041W	N	N
YOR197W	P	C	YDR189W	N	C
YBR143C	P	C	YNL049C	P	C
YML097C	N	C	YBL099W	N	MITO
YER043C	N	C	YNL121C	N	MITO
YOL016C	N	C	YHR117W	N	MITO
YGR254W	N	C	YFR051C	N	C
YMR220W	P	C	YMR011W	N	M
YHR174W	N	C	YJR121W	N	MITO
YHR111W	N	C	YBR127C	N	C
YER178W	N	MITO	YNL064C	N	C
YOL059W	N	C	YMR079W	P	C
YOR230W	N	N	YLR447C	N	C
YOR375C	P	C	YKL166C	P	N
YPL245W	N	C	YML008C	P	C

YPL145C	P	C	YCR021C	N	M
YOR209C	N	C	YKL080W	N	C
YGR285C	N	C	YGR028W	N	MITO
YOL097C	N	C	YIL076W	N	C
YPR108W	N	N	YOR074C	N	M
YLR438W	N	C	YNL055C	P	
YNL220W	N	C	YFL045C	P	C
YPR148C	N	C	YPR149W	N	M
YKL181W	P	C	YJL024C	N	C
YOL058W	P	C	YPL010W	N	C
YOR117W	N	N	YDL192W	N	C
YDL029W	N	C	YGR082W	N	MITO
YDR394W	N	MITO	YGR020C	N	M
YNL207W	P	C	YLR110C	N	N
YGR234W	N	C			

Discussion

In this study, we find out another new pathway that cell deal with misfolded proteins. After acute stress, the heat shock induced protein aggregates are imported in to mitochondria for degradation. This contributes to maintain the whole cell proteostasis. Disrupt of mitochondria protease system will delay the degradation of protein aggregates. The two disease related protein also showed interaction with mitochondria.

One thing we could find out is that what percentage of this pathway contribute to the proteostasis when dealing with acute stress induced protein aggregates. If we block other proteostasis systems, how long the dissolution of the aggregates will take.

Refolding and recycling of misfolded proteins are always went through the help of chaperones. What's the role of the chaperones like HSP104 and HSP70 in this process is also worth looking at. HSP104, which is a protein disaggregase, could be the most important chaperone in this process.

As an eukaryotic cell, budding yeast works as a nice model protein to study basic bioscience. The pathway we find in yeast could also be interesting to see if it remains true in mammalian cells.

Compare to the early findings[23-25] which the TDP43 orα-synuclein were expressed under Gal inducible promoter, the strong promoter GAP seems give us a different phenotype. Also under different metabolism activity, the maintenance of proteostasis could be totally different. The growth of yeast cells are totally inhibited by the over expression of α-synuclein.

References

1 Hartl, F. Ulrich, Andreas Bracher, and Manajit Hayer-Hartl. "Molecular chaperones in protein folding and proteostasis." *Nature* 475.7356 (2011): 324-332.

2 Tyedmers, Jens, Axel Mogk, and Bernd Bukau. "Cellular strategies for controlling protein aggregation." *Nature reviews Molecular cell biology* 11.11 (2010): 777-788.

3. Heinemeyer, W., P. C. Ramos, and R. J. Dohmen. "Ubiquitin-proteasome system." *Cellular and molecular life sciences* 61.13 (2004): 1562-1578.

4 Nakatogawa, H., Suzuki, K., Kamada, Y. & Ohsumi, Y.Dynamics and diversity in autophagy mechanisms:lessons from yeast. *Nature Rev. Mol. Cell Biol.* 10,458–467 (2009).

5 Ross, C. A. & Poirier, M. A. Protein aggregation and neurodegenerative disease. *Nature Med.* **10**,S10–S17 (2004).

6 Guo, Weirui, et al. "An ALS-associated mutation affecting TDP-43 enhances protein aggregation, fibril formation and neurotoxicity." *Nature structural & molecular biology* 18.7 (2011): 822-830.

7 Baba, Minami, et al. "Aggregation of alpha-synuclein in Lewy bodies of sporadic Parkinson's disease and dementia with Lewy bodies." *The American journal of pathology* 152.4 (1998): 879.

8 Lashuel, Hilal A., et al. "The many faces of α-synuclein: from structure and toxicity to therapeutic target." *Nature Reviews Neuroscience* 14.1 (2013): 38-48.

9 Outeiro, Tiago Fleming, and Susan Lindquist. "Yeast cells provide insight into alpha-synuclein biology and pathobiology." *Science* 302.5651 (2003): 1772-1775.

10 Bendor, Jacob T., Todd P. Logan, and Robert H. Edwards. "The function of α-synuclein." *Neuron* 79.6 (2013): 1044-1066.

11 Zhou, C. *et al.* Organelle-based aggregation and retention of damaged proteins in asymmetrically dividing cells. *Cell* **159**, 530-542, (2014).

12 Gupta, Rajat, et al. "Firefly luciferase mutants as sensors of proteome stress." *Nature methods* 8.10 (2011): 879-884.

13 Ruan, Linhao, et al. "Cytosolic proteostasis through importing of misfolded proteins into mitochondria." *Nature* 543.7645 (2017): 443-446.

14 Boldogh, I. R. & Pon, L. A. Purification and subfractionation of mitochondria from the yeast Saccharomyces cerevisiae. *Methods in cell biology* **80**, 45-64 (2007).

15 Ru, Qinhua Cindy, et al. "Proteomic profiling of human urine using multi-dimensional protein identification technology." *Journal of Chromatography A*1111.2 (2006): 166-174.

16 Huh, Won-Ki, et al. "Global analysis of protein localization in budding yeast."*Nature* 425.6959 (2003): 686-691.

17 Ashburner, Michael, et al. "Gene Ontology: tool for the unification of biology."*Nature genetics* 25.1 (2000): 25-29.

18 Cabantous, Stéphanie, Thomas C. Terwilliger, and Geoffrey S. Waldo. "Protein tagging and detection with engineered self-assembling fragments of green fluorescent protein." *Nature biotechnology* 23.1 (2005): 102-107.

19 Martin, J., Mahlke, K. & Pfanner, N. Role of an energized inner membrane in mitochondrial protein import. Delta psi drives the movement of presequences. *The Journal of biological chemistry* **266**, 18051-18057, (1991).

20 Chaudhari AA et al. Mitochondrial transmembrane potential and reactive oxygen species generation regulate the enhanced effect of CCCP on TRAIL-induced SNU-638 cell apoptosis. J Vet Med Sci 70:537-42 (2008)

21 Baker, M. J., Tatsuta, T. & Langer, T. Quality control of mitochondrial proteostasis. Cold Spring Harb Perspect Biol 3 (2011).

22 Van Dijl, Jan Maarten, et al. "The ATPase and protease domains of yeast mitochondrial Lon: roles in proteolysis and respiration-dependent growth."*Proceedings of the National Academy of Sciences* 95.18 (1998): 10584-10589.

23 Johnson, Brian S., et al. "A yeast TDP-43 proteinopathy model: Exploring the molecular determinants of TDP-43 aggregation and cellular toxicity."*Proceedings of the National Academy of Sciences* 105.17 (2008): 6439-6444.

24 Outeiro, Tiago Fleming, and Susan Lindquist. "Yeast cells provide insight into alpha-synuclein biology and pathobiology." *Science* 302.5651 (2003): 1772-1775.

25 Tardiff, Daniel F., et al. "Yeast reveal a “druggable” Rsp5/Nedd4 network that ameliorates α-synuclein toxicity in neurons." *Science* 342.6161 (2013): 979-983.

Erli Jin Resume

Education

Bachelor: East China University of Science and Technology, Shanghai, P. R. China
Major: Bioengineering (Bachelor of Engineering)
GPA: 3.48/4.00
Master: Johns Hopkins University, Baltimore, Maryland, United States of America
Major: Chemical and Biomolecular Engineering (Master of Science in Engineering)(expected May 2017)
GPA:3.58/4.00

Awards and Honors

2014.10: 3rd Academic Scholarship in Comprehensive Courses, awarded by East China University of Science and Technology
2013.10: School Excellent Student, awarded by East China University of Science and Technology
2013.10: B-Level Excellent Social Worker, awarded by East China University of Science and Technology
2013.10: 2nd Academic Scholarship in Comprehensive Courses, awarded by East China University of Science and Technology
2012.10: 3rd Academic Scholarship in Comprehensive Courses, awarded by East China University of Science and Technology
2016.09: ChemBE Master's Essay Scholarship for fall 2016 and spring 2017 semester awarded by Johns Hopkins University

Research Experience

01/2016~Present: Proteostasis under acute stress
-- Build model for study proteostasis under acute stress
-- Used *in vitro* and *in vivo* methods to study misfolded proteins' composition and dissolution
-- Studied mitochondria's role in dealing with misfolded proteins
-- Ruan, Linhao, Chuankai Zhou, **Erli Jin**, Andrei Kucharavy, Ying Zhang, Zhihui Wen, Laurence Florens, and Rong Li. "Cytosolic proteostasis through importing of misfolded proteins into mitochondria." *Nature* 543, no. 7645 (2017): 443-446.

11/2014~05/2015: Core-shell Molecular Imprinting Technology for Separating Lincomycin A
-- Undergraduate thesis

-- Made Lincomycin A specialized core-shell imprinting molecules

-- Used HPLC to purify Lincomycin A

10/2011~03/2014: University Students Innovation Program, Shanghai Area, East China University of Science and Technology
-- Responsible for municipal-level program: the separation of vitamin B12 by using the two-phase aqueous system

-- Program Leader,Coordinated between team member and the program instructors

-- Conducted experiments and made records and analysis

Internship& Extracurricular Activities

10/2012~06/2014: Students Representative Practice Committee, East China University of Science and Technology

-- Served as the consultant of the Committee

-- Responsible for conducting new students questionnaires and reporting the feedbacks

-- Invited professors for lectures on specific hot themes such as interviews and the software teaching

-- Assisted in monthly student meetings and organized the campus activities such as planting trees to promote environment

07/2012~08/2012: Shanghai Rui Bang Industrial Co., Ltd, Shanghai

-- Worked as the technician in the Technology Department

-- Assisted in the producing and the testing of the products and learned to use the Auto CAD software

-- Got familiar with the working conditions and learned the importance of being professional

2010: The 23th Shanghai Brains Olympic Innovative Competition, Shanghai

-- Volunteer in the competition area

-- Kept orders and guide the competitors

-- Realized the importance of the school spirit